sustainability

MDPI

Article

Optically Modulated Passive Broadband Daytime Radiative Cooling Materials Can Cool Cities in Summer and Heat Cities in Winter

Ansar Khan [1], Laura Carlosena [2,*], Jie Feng [3], Samiran Khorat [4], Rupali Khatun [5], Quang-Van Doan [6] and Mattheos Santamouris [3]

1 Department of Geography, Lalbaba College, University of Calcutta, Howrah 711202, India; khanansargeo@gmail.com
2 Department of Engineering, Arrosadia Campus, Public University of Navarra (UPNA), 31006 Pamplona, Spain
3 Faculty of Built Environment, University of New South Wales, Sydney, NSW 2052, Australia; jie.feng@unsw.edu.au (J.F.); m.santamouris@unsw.edu.au (M.S.)
4 Department of Geography, University of Calcutta, Kolkata 700019, India; samirankhorat054@gmail.com
5 School of Environmental Studies, Jadavpur University, Kolkata 700032, India; rupaliocean@gmail.com
6 Centre for Computational Sciences, University of Tsukuba, Tsukuba 305 8577, Ibaraki, Japan; doan.van.gb@u.tsukuba.ac.jp
* Correspondence: laura.carlosena@unavarra.es

Abstract: Broadband passive daytime radiative cooling (PDRC) materials exhibit sub-ambient surface temperatures and contribute highly to mitigating extreme urban heat during the warm period. However, their application may cause undesired overcooling problems in winter. This study aims to assess, on a city scale, different solutions to overcome the winter overcooling penalty derived from using PDRC materials. Furthermore, a mesoscale urban modeling system assesses the potential of the optical modulation of reflectance (ρ) and emissivity (ε) to reduce, minimize, or reverse the overcooling penalty. The alteration of heat flux components, air temperature modification, ground and roof surface temperature, and the urban canopy temperature are assessed. The maximum decrease of the winter ambient temperature using standard PDRC materials is 1.1 °C and 0.8 °C for daytime and nighttime, respectively, while the ρ+ε-modulation can increase the ambient temperature up to 0.4 °C and 1.4 °C, respectively, compared to the use of conventional materials. Compared with the control case, the maximum decrease of net radiation inflow occurred at the peak hour, reducing by 192.7 Wm^{-2} for the PDRC materials, 5.4 Wm^{-2} for ρ-modulated PDRC materials, and 173.7 Wm^{-2} for ε-PDRC materials; nevertheless, the ρ+ε-modulated PDRC materials increased the maximum net radiation inflow by 51.5 Wm^{-2}, leading to heating of the cities during the winter.

Keywords: urban heat mitigation; broadband radiative cooling emitters; overcooling; optical modulation; WRF-SLUCM; Kolkata

Citation: Khan, A.; Carlosena, L.; Feng, J.; Khorat, S.; Khatun, R.; Doan, Q.-V.; Santamouris, M. Optically Modulated Passive Broadband Daytime Radiative Cooling Materials Can Cool Cities in Summer and Heat Cities in Winter. *Sustainability* **2022**, *14*, 1110. https://doi.org/10.3390/su14031110

Academic Editors: Steve Kardinal Jusuf, Soh Chew Beng, Elsa Feng and Szu-Cheng Chien

Received: 19 December 2021
Accepted: 15 January 2022
Published: 19 January 2022

1. Introduction

1.1. Context

Extreme urban heat is the most documented phenomenon of climate change. It is related to higher ambient temperatures in dense urban areas compared to the surrounding suburban and rural areas [1]. The phenomenon is experimentally documented in more than 450 cities worldwide, and its magnitude may be as high as 10 °C [2,3]. Higher urban temperatures significantly influence energy use, ambient air, and health, augmenting cooling energy consumption and increasing peak power demand, pollutant concentrations, and heat-related morbidity and mortality [4–6].

To counterbalance the impact of urban overheating, several heat mitigation technologies have been researched and implemented. Moreover, urban design plays an important

role. The orientation and geometry of streets directly affect the solar access and airflow in urban canyons and, thus, the pedestrians' thermal comfort [7]. According to research, canyon thermal conductance rises linearly with wind intensity, making larger streets more vulnerable to thermal losses [8]. Empirical research found that the natural ventilation capacity in buildings located inside urban canyons was severely limited for both single-side and cross ventilation arrangements [9]. Among the various technologies researched to overcome urban overheating, the use of evaporative systems, additional green infrastructure, and significantly advanced materials seem to present a higher cooling potential [10]. Advanced materials for use in the urban fabric and outdoor spaces, including reflective, chromic, fluorescent, and photonic coatings, can seriously reduce the ambient temperature of cities and counterbalance the impact of urban heating [11]. Passive daytime radiative cooling (PDRC) materials present a high reflectance in the solar spectrum and a high emissivity value in the atmospheric window (8–13 μm). As a result, they can exhibit sub-ambient surface temperatures under the sun and greatly contribute to mitigating urban heat [12]. Thus, they are a great source of passive cooling since buildings require the highest cooling loads during the peak hours of the day. The research and development of PDRCs have grown tremendously in the last decade.

Nevertheless, spectrally selective materials entail a very complex design process since they have differentiated optical properties along the spectrum, with some areas showing absorption or emission and others exhibiting high reflectance. Therefore, several research overviews have covered the intrinsic design of various materials proposals in detail. The main issues include concerns related to climate adequation, the type of application (passive versus active), material development, the overcooling penalty, cost, scalability, and tunability.

To meet the stringent spectroscopic requirement for effective daytime radiative cooling, precise laboratory-based designs were developed using mainly photonic crystals and metamaterials. More recently, amorphous photonic structures, which use specific chemical bonds, have narrowed the gap towards mass production. Since the experiment of Raman et al. in 2014 [13] that achieved a 4 °C sub-ambient temperature reduction in Stanford (CA, USA), several photonics designs using the optimized integration of emitters and reflectors have subsequently been proposed [14–16]. For the time being, due to the cost and technical difficulties inherent in large-scale precise lithography, most photonic structures either remain as theoretical designs or cannot be mass-produced outside the laboratory. Compared with the precisely tailored photonic structures, the implementation of random photonic coolers has significantly reduced the cost and manufacturing sophistication of cooling systems without reducing the cooling performance. A low-cost emitter using random photonic media based on paint-format silicon dioxide (SiO_2) microspheres demonstrated unprecedented radiative cooling efficiency [17]. The coating, tested in Albuquerque (NM, USA), achieved a temperature reduction of 7 °C and an average of 4.7 °C below the substrate using the commercial paint. With an incident solar radiation of 1000 Wm^{-2}, the material achieved a cooling power of 100 Wm^{-2}.

Due to their mass manufacturing capabilities, competitive cost, and applicability to large systems, polymer-based radiative cooling films and paints have recently garnered interest. [18]. The authors tested two different polymers (PVDF and PMMA), applied on top of silver mirrors, in Boulder (CO, USA), achieving a temperature reduction between 6 °C and 4 °C during the day, respectively. Another team developed a metamaterial film [19] made of a glass-polymer hybrid material that achieved a cooling power of 93 Wm^{-2} under direct sunlight at noon in Cave Creek (AZ, USA). They integrated this metamaterial into a system to generate "free cooling," reducing energy consumption. Moreover, low-cost (0.3 €/m^2 for a layer of 2 μm) scalable, and sprayable polymeric materials with embedded SiO_2 particles were tested under a non-ideal environmental setting; the temperature of the bare substrate was reduced by 1.7 °C, with temperature decreases of up to 12 °C [20]. As opposed to the previous trials, this experiment took place in a temperate climate, Cfb using the Köppen–Geiger classification, near Pamplona (Spain) under changing weather conditions.

Paints used in another study were chosen for their easy and scalable application properties based on a hierarchically porous poly (vinylidene fluoride-co-hexafluoropropene) and were tested at several locations [21]. A 6 °C temperature reduction and a cooling power of 96 Wm^{-2} were found in Phoenix (AZ, USA); a cooling power of 83 Wm^{-2} was observed in New York (NY, USA); and a temperature drop of 3 °C was noted in Chattogram (Bangladesh), where fog and haze impeded the radiative heat loss into the sky. Finally, a 7.3 °C sub-ambient temperature drop was reported at noon in Beijing (China) by spraying zinc phosphate sodium onto aluminum [22].

Depending on their emissivity properties, PDRC materials are divided into two types: (a) broadband emitters with close-to-unity emissivity for all infrared wavelengths and (b) wavelength-selective emitters with a high emissivity only at the atmospheric window. The latter is well accepted as the ideal selective emitter with the best cooling performance under various climates; it can provide substantial temperature reduction of the ambient temperature [23]. However, when the material is warmer than the ambient air, or when its sub-ambient surface temperature is within the range of several degrees (the specific value varies with the climate), the broadband emitters can outperform the selective emitters due to the atmospheric windows [24]. Therefore, the development of low-cost, durable broadband radiative coolers can provide excellent benefits for large-scale applications.

It must be noted that the experiments with PDRC materials are usually conducted at locations with high sky view factors; as a result, they are not affected by incoming solar energy from buildings. This kind of experiment might lead to an overestimation of the cooling potential under actual city environments. Therefore, simulations are needed to calculate their cooling potential and overcooling penalty in urban environments. Few studies have researched the implication of their use at the city scale, especially on a street scale. Bartesaghi-Koc et al. compared numerous mitigation measures on an urban street canyon, concluding that implementing PDRC materials on shading devices was one of the most effective solutions tried in the study, lowering the ambient temperature by up to 1.6 °C and the surface temperature by 24.2 °C [25].

The use of PDRC materials will increase the summertime energy savings compared to the use of conventional reflective materials and will significantly improve the thermal balance of the cities [26]. Nevertheless, if substantial sub-ambient temperature is achieved, it can lead to unwanted outcomes such as condensation. Moreover, the application of broadband radiative cooling materials in the urban fabric may cause an overcooling penalty and increase the energy consumption for heating purposes. According to recent research, the widespread use of PDRC materials might drop city temperatures and reduce thermal comfort in winter, resulting in a daytime penalty of up to 186 Wm^{-2} [27].

1.2. Optical Modulation of Passive Daytime Radiative Cooling

To avoid unwanted winter cooling, modulation of the materials' spectra is needed. By switching the emissivity or reflectance to low values during the winter and high values during the warm period, PDRC materials may provide both heating and cooling benefits to cities. Inorganic thermochromic materials [28,29] and electrochromic materials [30] can achieve the dynamic modulation of emissivity. The most significant interest in thermochromic materials that change the emissivity spectrum has been in the development of the transition metal oxides that exhibit discontinuous changes in electrical conductivity of up to eight orders of magnitude. Vanadium dioxide is one of the most-researched metal oxides due to its characteristic phase transition at 68 °C, which is closest to ambient. Although closest to ambient, it is still a high-transition temperature for built environment applications. Therefore, research [31] has focused on lowering its transition temperature by doping with tungsten (W), molybdenum (Mo), tantalum (Ta), and niobium (Nb). A thin film, based on silicon monoxide, combined with a thermochromic layer, made of vanadium dioxide, was able to both cool and heat [32], achieving a stable temperature throughout the testing period.

Although the development of VO_2 has proven to be challenging, recent research has focused on simplifying and improving the expansion of techniques for different types of applications. For example, some authors focused on a simple, low-cost oxidation strategy for developing vanadium dioxide thin films [33], while others have synthesized VO_2 through an easy one-step annealing method [34]. In addition, others have investigated different ways to improve the process using the sol-gel technique, analyzing the importance of several precursors, such as scCO2 and imidazolium ILs, on polycondensation for the formation of vanadium gels [35]. Moreover, other authors have researched the use of different matrices to improve the lifespan of vanadium dioxide (VO_2) nanoparticles. For example, the highly entangled and crosslinked poly (methyl methacrylate) (PMMA) showed a promising pathway toward creating environmentally stable and easily scalable thermochromic films [36]. More recently, the VO_2 was doped with tin (Sn), enhancing its visible transmittance and providing the films with excellent thermochromic properties [37].

Reflectance modulation techniques are mainly based on commercially available thermochromic leuco-dyes. Their solar spectrum is absorbent in the color phase and highly reflective in the colorless phase. They can be absorbent during cold periods and reflective during hot seasons, thus decreasing the built environment's energy consumption in any season [38,39]. The application of leuco-dyes has been proven by including commercially available pigments in mortar. The solar reflectivity of the mortar increased in the visible spectrum while maintaining its reflectance values in the near-infrared area [40].

Selected research has pointed out materials that can modulate solar reflectivity and infrared emissivity to counteract unwanted overcooling. For example, a PDRC material that integrated an asymmetric electromagnetic transmission window theoretically achieved reflectance and emissivity modulation [41]. Another detailed demonstration of the effectiveness of modulation showed a large tunability for solar reflectance, mid-wave infrared emittance, and longwave infrared emissivity [42] using electrochromism. Finally, wet/dry chromism seen in some porous polymer coatings can be employed for dynamic light and heat management, as their solar and infrared transmittance alters when wetted by a particular liquid, indirectly changing the solar reflectance and emissivity simultaneously [43]. The use of these materials achieved sub-ambient radiative cooling (by 3.2 °C) and above-ambient solar heating (by 21.4 °C).

Recent empirical research reveals the conception of some very promising tunable radiative coolers. A temperature-adaptive radiative coating using vanadium dioxide doped with tungsten increased the thermal emittance from 0.20 for ambient temperatures lower than 15 °C to 0.90 for temperatures above 30 °C [44]. Moreover, a radiative coating applied over an aluminum plate achieved 6 °C below the ambient temperature under a solar intensity of 744 Wm^{-2}, yielding a cooling power of 84.2 Wm^{-2} [45]. New switchable materials for windows showed the modulation of longwave infrared emissivity of between 2.5 and 25 μm. In this application, vanadium dioxide nanoparticles were dispersed on a poly (methyl methacrylate) (PMMA) lossless spacer and two layers of indium tin oxide (ITO). This proved to be especially suitable for self-adapting applications across different climate zones. Moreover, simulations showed savings up to 324.6 MJm^{-2}, compared to results using commercial low-E glass [46].

Once the issue of winter overcooling has been presented and some feasible solutions to overcome it have been suggested, it is worth studying and quantifying the overcooling reduction that could be achieved using the different types of modulations (solar reflectance modulation, infrared emissivity modulation, and the modulation of both optical ranges). Therefore, the following questions should be addressed:

1. What is the impact of modulated and non-modulated PDRC materials on a city scale during the winter period?
2. How is the thermal balance maintained to avoid extra heating energy costs?
3. Once optical modulation techniques are applied, how much is the overcooling penalty reduced?

The main aim of this study is to investigate the overcooling penalty reduction by introducing different modulation techniques for the use of PDRC materials during the cold period and their effect on a city scale. The specific objectives are:

1. To present and discuss different technologies available to modulate the PDRC materials' optical characteristics to reduce the overcooling penalty.
2. To evaluate the potential to minimize the overcooling penalty in winter using the different optical modulation techniques.

2. Materials and Methods

To assess the impact of modulated and non-modulated PDRC materials on the urban climate, a control scenario, one standard non-modulated PDRC materials scenario, and three modulated PDRC materials scenarios are evaluated and presented. The ambient temperature, roof temperature, urban canopy temperature, sensible heat, latent heat, heat storage, and net inflow radiation are assessed (both day and night). The use of novel mitigation technologies, combined with modulation, is predicted to dramatically minimize temperatures. To the best of our knowledge, this is the first time that the thermal performance of standard and modulated PDRC materials will be assessed, and their impact on urban climatic characteristics evaluated, at a city scale during the winter period.

2.1. Climate and Location Selection

The Kolkata Metropolitan Area (KMA) was chosen as the location for studying the tropical regional context. KMA has a tropical wet and dry climate (Köppen–Geiger classification: Aw, tropical savanna climate), one of the most common climate in the equatorial regions. Moreover, the Intergovernmental Panel on Climate Change (IPCC) selected Kolkata among the urban areas for possible study, showing that the global near-surface temperature trend rose 2.6 °C in that location from 1950–2018 [47]. Besides, other researchers [48,49] have found increased temperatures observed in the KMA in the last century. As a result, the KMA would benefit from applying passive cooling technologies. In addition, it was selected because previous research [50] has shown that it would profit from the use of passive daytime radiative coolers during the summer. A recent study determined a high overcooling penalty due to using PDRC materials during winter [27]. Thus, the impact of using the different modulation techniques in winter was assessed in the same location. The models were simulated under a clear sky and a calm wind environment during two successive days (from December 21 to December 22, 2019) near the winter solstice in the KMA. The selected days are the shortest of the year. As a result, the materials are exposed to darkness for a more extended period; potentially these are the days with the highest overcooling due to outgoing radiation. A control case, one non-modulated scenario, and three modulated scenarios were simulated. For the chosen timeframe, the minimum and maximum temperatures were 14.5 °C and 24.2 °C, respectively. The average relative humidity was 57.8% and the average UHI was 3.1 °C with a high temperature of 5.6 °C and the low temperature of 0.6 °C.

2.2. Model Configuration

As accomplished in previous research, to explore the performance of several newly developed PDRC materials as heat mitigation technologies, the community Weather Research and Forecasting model (WRF v4.0.0) [51], coupled with the refined single-layer urban canopy model (SLUCM), was employed [52,53]. The WRF-SLUCM was set up with a parent domain (Domain 01) and two nested domains (Domain 02 and 03), each centered in Kolkata (22.57° N, 88.36° E). The Kolkata metropolitan region is centered over the innermost domains, and the spatial resolutions are 18 km, 6 km, and 2 km for Domain 01, 02, and 03, sequentially, as shown in Figure 1. The simulations were run using a server (High-Performance Computing System).

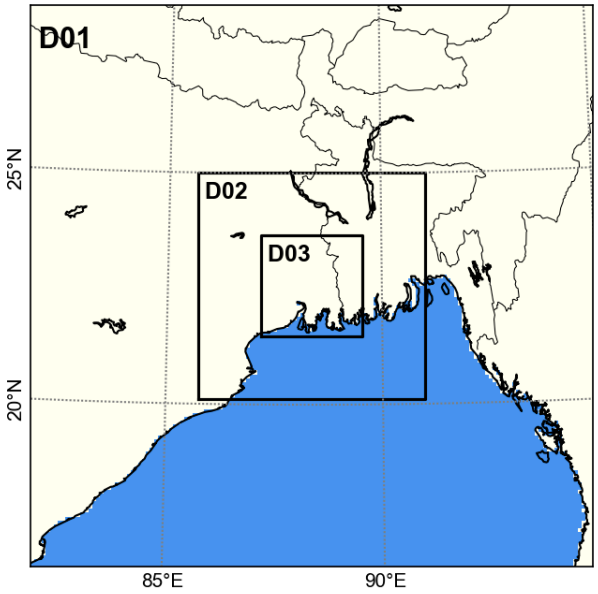

Figure 1. The WRF model configuration showing three domains. The parent domain, D01, has a horizontal grid spacing of 18 km, D02 with 6km grid spacing, and D03 indicates the inner domain of the area of interest which encompasses high-density urban of Kolkata metropolitan area (KMA) and has a grid spacing of 2 km.

On a 0.25 × 0.25-degree resolution grid, the high-resolution meteorological boundary conditions for the WRF-SLUCM planned for every three hours up to 240 h were procured from the Global Forecasting System (GFS) operational global analysis and forecast datasets provided by the National Centers for Environmental Prediction (NCEP) (2015). The physical WRF parameterization model used incorporates the Dudhia scheme [54] for shortwave radiation, the rapid radiative transfer model [55] for longwave radiation, the Purdue–Lin scheme [56] for the microphysics, the Mellor–Yamada TKE scheme [57] for the turbulence, the Kain–Fritsch (KF) scheme [58] for the cumulus parameterization, the Asymmetrical Convective Model, version 2 [59] for the planetary boundary layer, and the Noah LSM single-layer urban canopy model [52,53] for the model surface layer. The first 24 h of the simulation were used as the model spin-up time and were left out of the analysis, as previous research showed that a 24 h period was enough to reach the model equilibrium, and this is well confirmed in previous studies for Kolkata [27]. As WRF usually provides the best forecasts for 24 or 48 h for any typical day, i.e., hot or cold, the simulation was conducted from 21 December to 23 December 2019, with a clear sky and calm wind. The performance of broadband radiative coolers was evaluated using hourly simulation data from the innermost area.

2.3. Model Validation and Assessment

During the assessment period, the hourly output of 2 m air temperature from the base case scenario was compared with data from local observation across the D03 urban grid cells to assess the WRF-SLUCM performance. In-situ meteorological measurements were gathered using an hourly meteorological dataset from Weather Kolkata (http://weatherkolkata.in/ accessed on 24 October 2020). For model assessment and verification, the Kolkata Municipal Corporation (KMC) used six meteorological stations across the many urban land-use types. The mean bias error (MBE), mean absolute error (MAE), root mean square error (RMSE), and correlation coefficient (r) for the hourly 2 m air temperature are compared statistically in Table 1.

Table 1. A comparison of simulation outputs with data from local weather stations.

Parameters	Local Meteorological Station					
	Alipore	**Ratan Babu Ghat**	**Shibpur**	**Palmer Bridge**	**Jora Bridge**	**Joka**
Correlation coefficient	0.8165	0.9687	0.9422	0.8634	0.8216	0.9326
Mean bias error	−2.1	−0.34	−0.89	−1.0	0.05	−0.54
Mean absolute error	−2.1082	−0.3385	−0.8889	−1.044	0.0454	−0.5429
Root mean square error	2.9	0.8	1.4	1.9	2.0	1.4
Index of agreement	0.81	0.98	0.95	0.90	0.89	0.95

The temperature measured at multiple sites was accurately captured by the combined WRF-SLUCM model (mean r = 0.89; mean bias = 0.81). The base case simulation created urban weather conditions statistically similar to those observed locally ($p < 0.05$). The ranges of MBE and RMSE of air temperature are −0.5 °C to 2.1 °C and 0.8 °C to 2.9 °C, respectively. Over the metropolitan grid, the best predictions of 2 m air temperature were found in the Ratan Babu Ghat (0.8 °C) urban grid. Nevertheless, the model underestimated the 2 m air temperature, likely due to the solar radiation inaccuracy above the KMA. Model biases were mainly driven by: (a) a lack of suitable urban morphological representation and (b) an uncertainty in the designs of the physical models, the input data used, and the model parameters. The range of index of agreement for the 2 m air temperature is 0.81 to 0.95 compared to the simulated result. This preliminary validation demonstrates that the model can accurately and realistically simulate the urban environment, and it may be helpful for further investigations related to urban heat mitigation measures.

2.4. Study Cases: Kolkata Metropolitan Area

Five specific scenarios were designed and assessed to evaluate the performance of PDRC materials as urban heat mitigation technologies during the winter period. One base case (control), one standard PDRC material, and three additional modulated PDRC material scenarios were simulated. The characteristics are summarized in Table 2. Initially, the control case with the default urban settings was set up to ensure that the model was reliable. The control values approximate Kolkata's construction environment, where the buildings' roofs are mainly made of reinforced concrete with dark-colored surfaces, and the roads are paved with asphalt with low albedo values from 0.10 to 0.35. The first scenario (nm-PDRC) implemented standard broadband PDRC materials for covering the roofs. Their reflectance and emissivity were selected according to values commonly reported in the literature [42]. The second scenario (ρ-PDRC) considered the reflectance modulation of the materials to a low value corresponding to an average reflectance of thermochromic materials during their color phase [60], while the emissivity remained the same as in scenario 1. The third scenario (ε-PDRC) considered that the emissivity of the materials was modulated, achieving a low value, as reported in [41], while the reflectance remained similar to that in the standard PDRC materials, scenario 1. Finally, the fourth scenario (ρ+ε-PDRC) considered both low solar reflectance (as in scenario 2) and low emissivity (as in scenario 3). After modulation, the assigned reflectance and emissivity values are indicative and close to the reported values. However, the existing literature on this topic is limited, so the use of switchable optical properties in practice may differ from the selected values. For all the scenarios, the optical properties of the walls and the ground remained unchanged.

Table 2. The WRF-SLUCM simulation of numerical design for the control case and the several types of PDRC broadband emitters under investigation.

Numerical Design	Type of Roof	Scenario	Optical Properties of the Material	
			Reflectance (ρ)	Emissivity (ε)
Control case (CTRL)	Conventional	Control scenario	Roof 0.20 Wall 0.20 Ground (road) 0.20	Roof 0.85 Wall 0.85 Ground (road) 0.85
Non-modulated (nm-PDRC)	Standard PDRC roof	Scenario 1	Roof 0.95 Wall 0.20 Ground(road) 0.20	Roof 0.93 Wall 0.85 Ground (road) 0.85
Reflectance modulated (ρ-PDRC)	ρ-modulated PDRC roof	Scenario 2	Roof 0.20 Wall 0.20 Ground(road) 0.20	Roof 0.93 Wall 0.85 Ground (road) 0.85
Emissivity modulated (ε-PDRC)	ε-modulated PDRC roof	Scenario 3	Roof 0.95 Wall 0.20 Ground(road) 0.20	Roof 0.20 Wall 0.85 Ground (road) 0.85
Reflectance and emissivity modulated (ρ+ε-PDRC)	ρ+ε-modulated PDRC roof	Scenario 4	Roof 0.20 Wall 0.20 Ground(road) 0.20	Roof 0.20 Wall 0.85 Ground (road) 0.85

Using mean values in the emissivity and reflectivity data might lead to overestimations or underestimations. On the one hand, an overestimation of the solar reflectivity might translate to the actual material heating substantially more than estimated. On the other hand, an overestimation of the infrared emissivity might cause the material to evacuate less heat than simulated. Moreover, the impact of the wavelength on the ability of the material to cool down or heat up depends significantly on the incoming radiation and the atmospheric transparency at that same wavelength. Sky models and climate data are crucial to determine the final thermal balance. Since heat is absorbed by water vapor at specific wavelengths, clouds and precipitable water vapor operate as a barrier to heat transmission, reducing outgoing radiation through the atmospheric band and increasing the effective temperature of the sky. Previous research conducted a sensitivity analysis on the impact of wavelength emissivity [61] and climate parameters [23] on the ability to achieve daytime radiative cooling.

3. Results

This section presents the performance of different PDRC broadband emitters (non-modulated, reflectance modulated, emissivity modulated, and reflectance and emissivity modulated) for a tropical wet and dry climate. The material's optical properties in the solar spectrum considerably balance the solar radiation absorbed by the urban faces and change the surface heat flux partition (according to the Bowen ratio for latent and sensible heat) over the urban surface. It can also impact the city-scale local convection by altering the moisture exchange between the urban surface and the lower atmosphere. The detailed results are presented and discussed below.

3.1. The Magnitude of Heat Flux and Net Inflow Radiation

Figure 2 depicts the heat flux components for the various numerical scenarios; sensible heat, latent heat, heat storage, and net inflow radiation were investigated and compared. Detailed results are shown in Table 3.

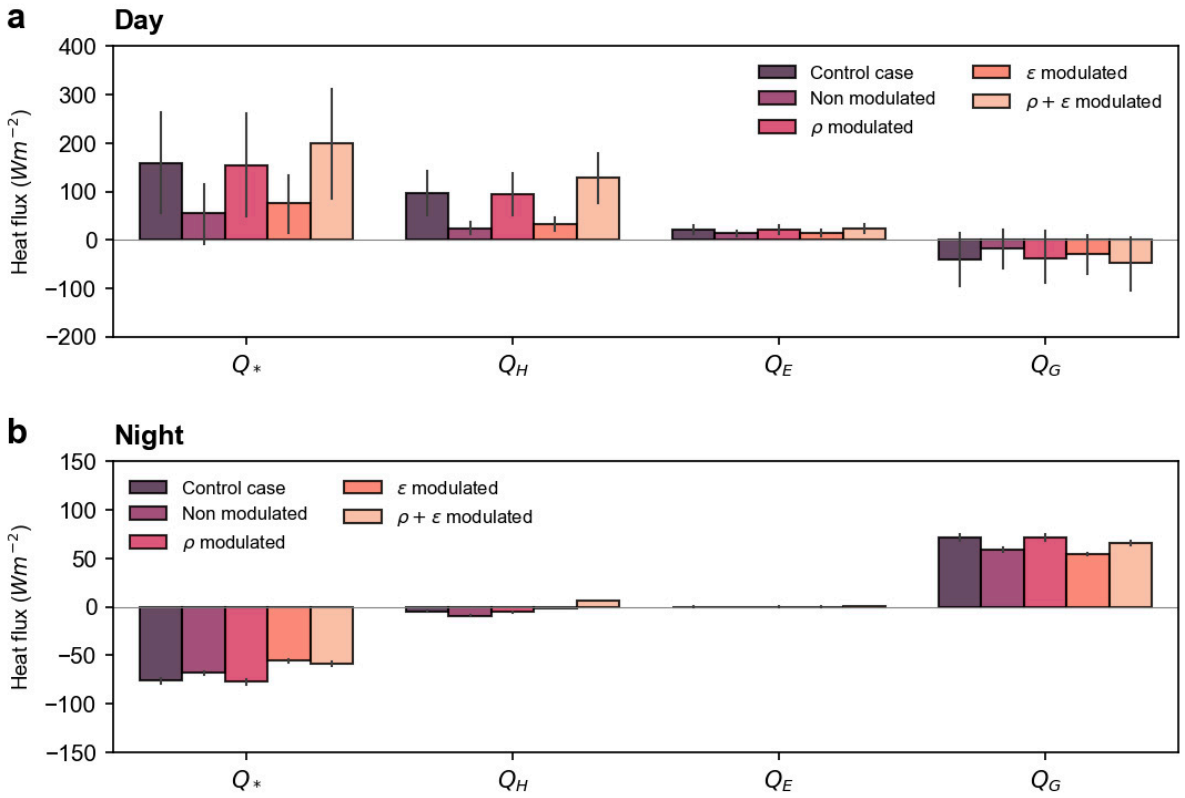

Figure 2. The surface energy heat flux simulations on a diurnal scale for a typical winter episode using PDRC materials and their modulations for D03. The differences in heat fluxes from WRF-SLUCM model simulations were derived from two-dimensional surface energy budget/radiation. Q_H, Q_E, Q^*, and Q_G denote the sensible heat, the latent heat, net inflow radiation, and heat storage, respectively, (**a**) shows the surface energy heat flux during the day and (**b**) represents the heat flux at night.

Table 3. The distribution of the flux parameters for the PDRC broadband emitters in the winter.

Heat Flux (Wm^{-2})		CTRL	nm-PDRC	ρ-PDRC	ε-PDRC	ρ+ε-PDRC
Q_H	Day max.	188.5	51.0	183.8	61.1	233.1
	Night max.	−1.1	−3.6	−1.5	2.0	6.4
	Day avg.	94.1	23.7	91.1	31.4	112.8
	Night avg.	−3.0	−6.4	−3.5	−1.0	5.2
Q_E	Day max.	58.5	44.6	58.4	45.1	59.8
	Night max.	18.2	18.3	18.2	16.8	16.8
	Day avg.	36.6	28.4	36.5	29.3	37.9
	Night avg.	0.5	0.6	0.6	0.7	0.9
Q_G	Day max.	86.5	70.9	87.6	59.9	78.7
	Night max.	76.8	61.6	77.7	54.1	66.2
	Day avg.	−41.6	−20.4	−40.9	−29.8	−48.7
	Night avg.	61.8	51.1	62.2	46.2	55.4
Q_E	Day max.	385.4	192.7	380.0	211.7	436.9
	Night max.	−37.7	−33.7	−38.4	−25.5	−28.5
	Day avg.	170.4	72.6	166.5	90.6	208.4
	Night avg.	−73.9	−66.4	−74.9	−52.2	−56.4

3.1.1. Change of Sensible Heat (Q_H)

The daily average sensible heat released under the current urban conditions (CTRL) was 94.1 Wm^{-2}, decreasing to 23.7 Wm^{-2} (74.8% reduction or 70.4 Wm^{-2} less) when standard PDRC materials were considered for the urban roofs (Figure 2a). Modulation of the material's reflectance (ρ-PDRC) decreased the average daily sensible flux up to 91.1 Wm^{-2}

(7.7% decrease from CTRL). When the materials' emissivity was modulated (ε-PDRC), the sensible heat increased slightly (32.5% or 7.7 Wm^{-2}) compared to the non-modulated PDRC material, but was considerably lower than the flux under the control conditions, showing an absolute value of 31.4 Wm^{-2}. However, when both the reflectance and emissivity were modulated (ρ+ε-PDRC), the daily average sensible heat release increased to 112.8 Wm^{-2} (an increase of 19.9% compared with the CTRL), highly contributing to heating the ambient environment. During the daytime, the standard PDRC materials had the greatest influence on Q_H reduction, since they stopped incoming radiation, and the input energy itself was lower over the urban area.

During the nighttime, when the reflectance, emissivity, or both were modulated, the average release of sensible heat increased by 2.9 Wm^{-2}, 5.4 Wm^{-2}, and 11.6 Wm^{-2}, respectively, compared to the non-modulated PDRC.

3.1.2. Change of the Latent Heat (Q_E)

The variation of the latent heat, for both day and night, was, as expected, not significant. Compared with the CTRL, the maximum decrease of latent heat was 13.9 Wm^{-2} for nm-PDRC and occurred at the peak hour (14:00 local time), representing a 23.8% reduction. The average daily mean of latent heat decrease was 8.2 Wm^{-2} for the nm-PDRC material compared to the CTRL (22.4% reduction). When the reflectance, emissivity, and both were modulated, the average daily mean of latent heat correspondingly increased by 8.1 Wm^{-2} (28.5%), 0.9 Wm^{-2} (3.2%), and 9.5 Wm^{-2} (33.5%) compared to the non-modulated PDRC material.

3.1.3. Change of the Net Inflow Radiation (Q^*)

The PDRC materials reduce the amount of solar energy absorbed by urban surfaces, which helps to reduce urban heat. The net inflow radiation Q^* also reduced during the daytime, and the greatest decline occurred at peak hours, coinciding with the maximum incident solar radiation. The maximum decrease of net radiation inflow occurred at the peak hour, reducing by 192.7 Wm^{-2} for the nm-PDRC, 5.4 Wm^{-2} for the ρ-PDRC, and 173.7 Wm^{-2} for the ε-PDRC. Nevertheless, when both the reflectance and the emissivity were modulated, the maximum net radiation inflow increased by 51.5 Wm^{-2} (ρ+ε-PDRC), compared to the CTRL. The net inflow radiation increased 97% (187.3 Wm^{-2}), 9.9% (19 Wm^{-2}), and 126% (244.2 Wm^{-2}) for the three modulated scenarios, respectively, compared with the non-modulated PDRC. During the nighttime, the average net inflow radiation increased from the CTRL by 7.5 Wm^{-2}, 21.7, and 17.5 for the nm-PDRC, the ε-PDRC, and the ρ+ε-PDRC, respectively, as opposed to the ρ-PDRC that decreased by 1 Wm^{-2}.

3.1.4. Change of the Heat Storage (Q_G)

The maximum increase in heat storage occurred at the peak hour, and similar values were attained by the CTRL and the ρ-PDRC, 86.5 Wm^{-2} and 87.6 Wm^{-2}, respectively. Conversely, compared to the standard PDRC, the daytime average heat storage decreased by 20.5 Wm^{-2}, 9.4 Wm^{-2}, and 20.3 Wm^{-2} for the reflectance-modulated, emissivity-modulated, and both modulated. In general, the reflectance-modulated scenario showed the most similar behavior compared with the control case, both during the day and night.

3.2. Change of Temperatures

Figure 3 shows the temperature variations (ΔT) in the different scenarios (non-modulated and modulated PDRC materials) and the CTRL case. The maximum and average $T_{ambient}$, $T_{surface}$, $T_{roof,}$ and T_{canopy} for both day and night are shown in Table 4.

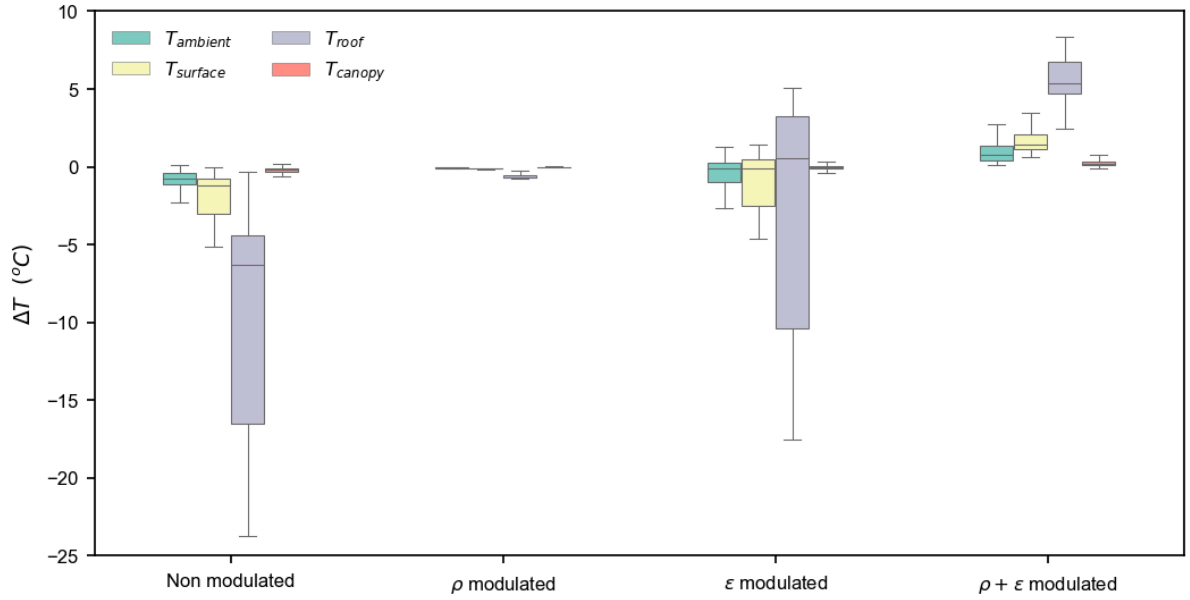

Figure 3. The temperature boxplots of the urban environment variables (hourly) over a high-density urban area where PDRC materials are deployed for D03. Results of 24 h × 169 points from scenarios (non-modulated and modulated PDRC materials) minus the control case (ΔT), for $T_{ambient}$, T_{roof}, $Ts_{urface,}$ and T_{canopy}. These temperatures were calculated using the energy budget on each facet's canyon surface (roof, wall, and ground) and their influence on heat fluxes.

Table 4. The distribution of thermal parameters for the different PDRC broadband emitters in winter.

Temperature (°C)		CTRL	nm-PDRC	ρ-PDRC	ε-PDRC	ρ+ε-PDRC
$T_{ambient}$	Day max.	24.2	23.1	24.2	23.3	24.6
	Night max.	21.5	20.7	21.5	21.3	22.9
	Day avg.	21.1	20.1	21.1	20.4	21.6
	Night avg.	17.9	17.3	17.8	18.0	19.2
$T_{surface}$	Day max.	27.0	23.8	26.9	24.1	27.9
	Night max.	21.2	20.1	21.1	21.0	22.9
	Day avg.	23.0	20.8	22.9	21.3	24.0
	Night avg.	17.8	17.0	17.7	18.1	19.7
T_{roof}	Day max.	35.7	16.4	35.3	21.8	40.0
	Night max.	19.6	13.4	19.0	19.7	24.8
	Day avg.	27.7	15.0	27.2	20.0	31.5
	Night avg.	15.6	11.2	15.0	18.0	21.6
T_{canopy}	Day max.	30.9	30.7	30.9	30.8	31.0
	Night max.	22.8	22.5	22.8	22.7	23.0
	Day avg.	25.5	25.3	25.5	25.2	25.6
	Night avg.	18.9	18.7	18.9	19.0	19.3
T_{air}	Day max.	23.3	23.0	23.0	23.0	23.4
	Night max.	22.3	21.5	22.1	22.1	22.8
	Day avg.	20.4	19.8	20.0	20.0	20.6
	Night avg.	18.5	18.0	18.6	18.6	19.5

3.2.1. Change of the Magnitude of the Ambient Temperature at 2 m Height ($T_{ambient}$)

Ambient temperatures at the 2 m height $T_{ambient}$ may be determined using the WRF-SLUCM urban modeling system's surface energy balance flux partitioning (Figure 3 and Table 4). The results showed that standard PDRC materials reduced the peak ambient temperature in the city by 2.6 °C compared to the control case. When the reflectance of the materials was modulated, the peak ambient temperature remained unchanged, as in the control case. However, modulation of the emissivity decreased the peak temperature by 1.5 °C compared

to the CTRL, while the modulation of both the reflectance and emissivity increased the peak ambient temperature by 0.8 °C and heated up the urban environment (Figure 4).

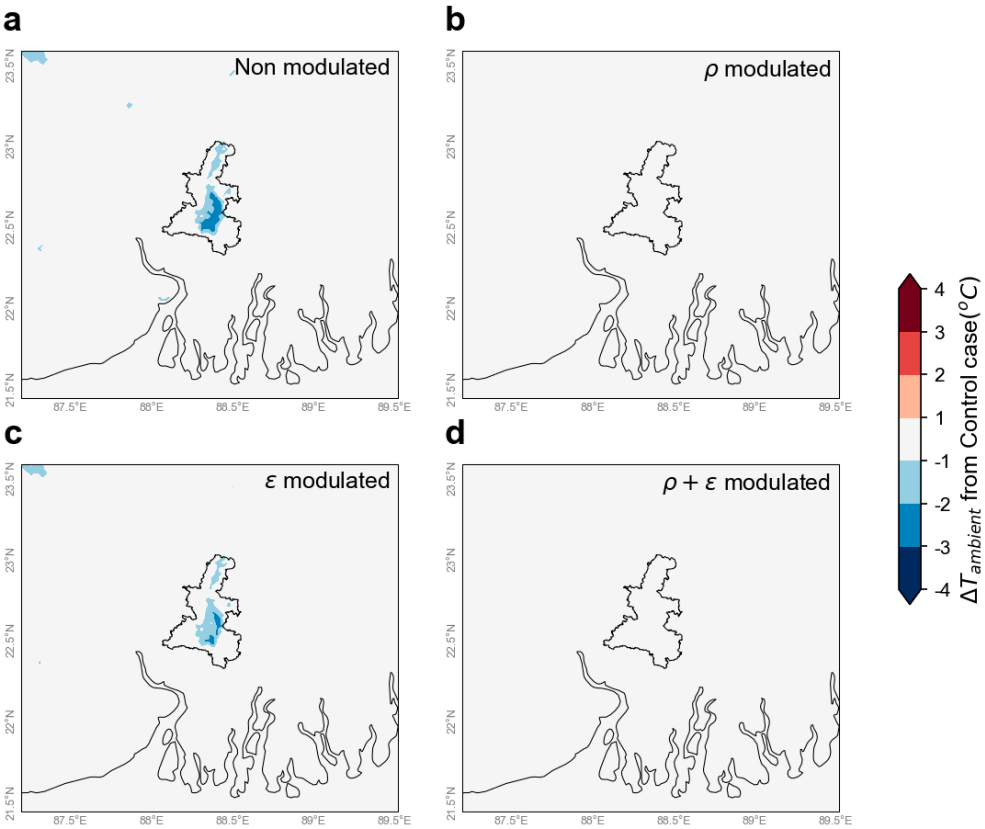

Figure 4. The drop of the $T_{ambient}$ temperature compared to the CTRL. The outcomes show that the temperature dropped in D03 in the high density-density residential Kolkata metropolitan area (KMA) where PDRC materials and their modulations were implemented during peak hours. In this case, (**a**) non-modulated PDRC materials significantly lowered the temperature due to the high reflectance and emissivity of the materials compared to the (**b**) ρ-modulated, (**c**) ε-modulated, and (**d**) ρ+ε-modulated materials. Nevertheless, the ρ-modulated and ρ+ε-modulated cases significantly reduced the cooling penalty more than the ε-modulated PDRC materials.

Consequently, the combined modulation of the optical properties (the ρ+ε-PDRC materials) presented the highest potential, increasing the average daily ambient temperature by 0.5 °C over the urban surface during the studied winter period. Single modulation of the reflectance also successfully reduced the winter overcooling penalty without any disadvantage, as the average of the daytime and nighttime $T_{ambient}$ variation was negligible and close to zero. During the daytime, the average $T_{ambient}$ reduction using conventional PDRC materials was 1.1 °C, while the average reduction during the nighttime was 0.6 °C.

Furthermore, the modulation of the emissivity decreased the average daytime temperature by 0.8 °C, but increased the average temperature during the night by 0.2 °C, compared to the control scenario. Finally, when both the reflectance and the emissivity were modulated, the average daily and nighttime ambient temperatures increased by 0.5 °C and 1.3 °C, respectively. When applied in the urban environment, the modulated PDRC materials could significantly reduce the peak summer temperature [50] while increasing the peak winter temperature, improving year-round thermal comfort conditions

3.2.2. Change in the Magnitude of the Ground Surface Temperature ($T_{surface}$)

When standard PDRC materials were used in the city, the maximum ground surface temperature ($T_{surface}$) decreased by nearly 4.9 °C compared to the control scenario (Figure 3). In parallel, the average day and nighttime reduction of the surface temperature was close to

2.2 °C and 0.8 °C (nm-PDRC), respectively. When the reflectance of the PDRC materials was modulated (ρ-modulated), the maximum and average reduction of the day and nighttime surface temperatures was meager, just 0.1 °C. The emissivity (ε-modulated) PDRC materials resulted in a maximum reduction of the day and nighttime surface temperatures by 2.9 °C and 0.2 °C, compared to the CTRL. The corresponding average daytime surface temperature reduction was 1.7 °C, as opposed to the nighttime temperature, where the average surface temperature increased by 0.3 °C. Finally, when both the optical properties were modulated (ρ+ε-modulated), the maximum surface temperature increased by 0.7 °C and 1.7 °C during the day and night, respectively, compared to the CTRL. As a result, the average day and nighttime surface temperatures for this scenario increased by 1 °C and 1.9 °C, respectively.

3.2.3. Change in the Magnitude of the Roof Surface Temperature (T_{roof})

When conventional PDRC materials were applied over the urban rooftops, the maximum decrease of the roof temperature (T_{roof}) at the peak hour was close to 22.8 °C, compared to the control case (Figure 3). When the reflectance of PDRC materials was modulated, the maximum and average temperature reduction during the daytime and nighttime was 0.3 °C. When the emissivity of the PDRC materials was modulated, the T_{roof} decreased by 19.5 °C at the peak hour compared to the control case. Nevertheless, when both optical properties were modulated (ρ+ε-PDRC), the T_{roof} increased by 8.6 °C during the peak hour and the average increases of the T_{roof} during the daytime and nighttime were 7.2 °C and 2.4 °C, respectively.

3.2.4. Change in the Magnitude of the Urban Canopy Temperature (T_{canopy})

Finally, the maximum urban canopy temperature (T_{canopy_max}), the ambient temperature above the roofs, was slightly reduced by 0.2 °C during the day and 0.3 °C during the night when conventional PDRC materials were considered, as opposed to the control case. The reflectance or emissivity modulation did not result in any considerable decrease or increase of the canopy temperature, while a combined modulation of both parameters (ρ+ε-modulation) slightly increased the canopy temperature by 0.1 °C or 0.2 °C.

3.3. Impact on the Lower Atmosphere

The objective of this assessment using modulated and non-modulated PDRC materials was to better understand the meteorology boundary layer and its representation in the mesoscale climate model for the winter season, a relatively unexplored research field. The results dealt with the performance of the different kinds of PDRC materials in modeling the lower-atmospheric thermodynamics and vertical kinematic profile for the urban domain in severely cold surroundings. Due to the application of a city-scale implementation of the PDRC materials, the meteorological conditions were changed. The lower degree of the effects buoyancy on an undiluted air parcel was discovered when PDRCs were imposed on the city during a cold night, possibly linked to the updraft strength of vertical convection, which was marginally reduced. The situation depends on whether any latent heat exists after freezing and whether the wet-adiabatic development is deemed reversible or irreversible in the PDRC's city. Because of the lack of convective accessible potential energy (CAPE) during the winter seasons, the PDRC's implemented city environment was in hydrostatic equilibrium, and the parcel's pressure was identical to that of the environment.

In general, the planetary boundary layer (PBL) began to rise on the south-facing elevations and near the ridges (which were first warmed up by sun and not deterred by cold air pockets generated on the valley overnight) and grew spatially from the afternoon to the nighttime. Convection halted around early evening, the lower atmosphere began to dissipate, and the average circulation proceeded to reverse into a sinking motion. Due to advection by the synoptic wind system controlled by the nearby southern sea and the northern long-range mountain, there was an insufficient residual layer at night. During the day, the PDRC materials reflected solar radiation, sending heat back to space and forming regional "high pressure" air enclosures over the urban environment. This phe-

nomenon was reflected in the near-surface wind, which was reduced by 2–3 ms^{-1} as the day progressed. The heat deficit resulted in a drop in ambient temperature across the metropolitan landscape.

Furthermore, in the urban atmosphere during winter, the offset of incoming solar radiation was a light energy source for creating the urban atmospheric mixing layer. When using PDRC materials, the simulated results for the KMA revealed that the consistently reduced temperature could not form an inversion layer. As shown in Figure 5, the prospective temperature showed those with a vertical profile for the boundary layer. These lower atmosphere meteorological shifts could result in a buildup of stagnant air above the urban areas. Subsequently, the stagnant air over the urban domain held the building's reflected heat and remained poised over the city for long hours. The stagnant air over the PDRC-implemented city could not be released as quickly into space, leading to nighttime heating during the winter period.

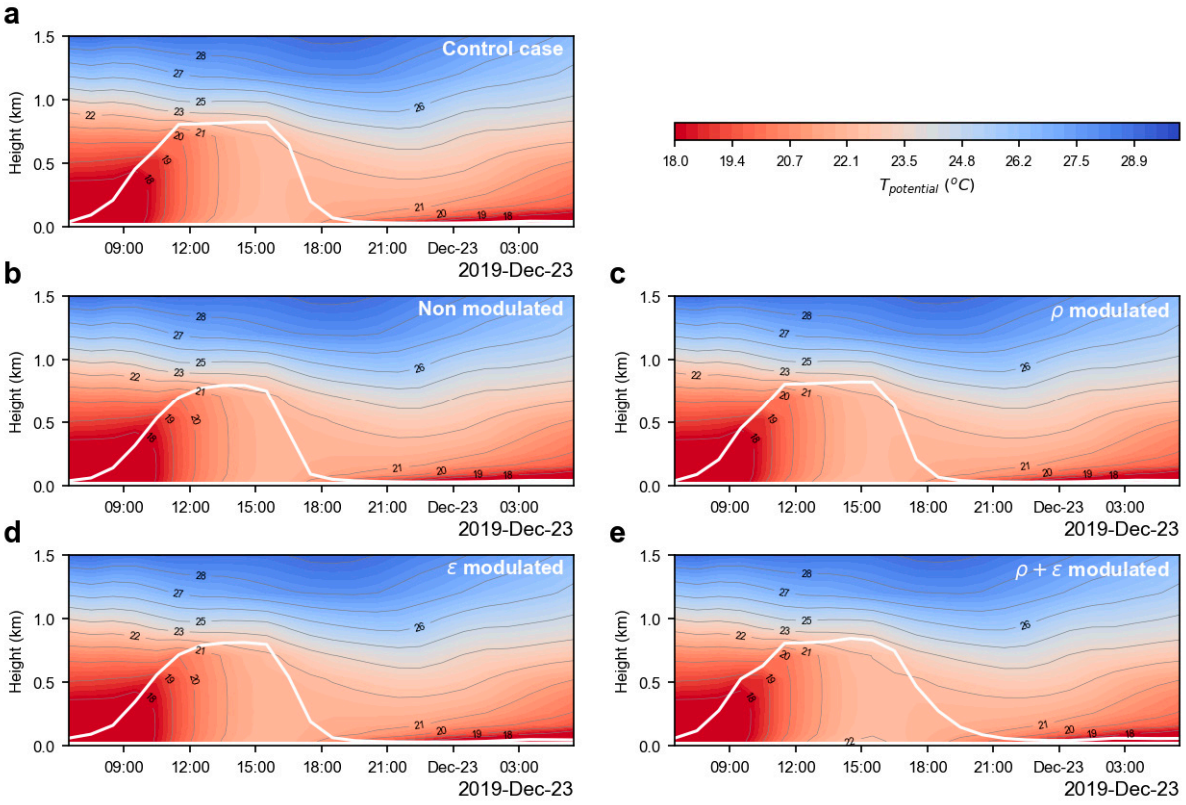

Figure 5. The changes in potential temperature over time in a city. The potential temperature during a diurnal cycle can assess the effects of the cooling of PDRC materials on boundary layer stability. The potential temperature remains constant when a parcel experiences an adiabatic pressure shift. The dry, static stability of the atmosphere is determined by the vertical gradient of the potential temperature. During the peak hour, the convective boundary layer grew the fastest and progressively balanced in the lower atmosphere with the (**a**) CTRL compared to the (**b**) non-modulated, (**c**) ρ-modulated, (**d**) ε-modulated, and the (**e**) ρ+ε-modulated PDRC materials. The modulated PDRC materials do not significantly affect the PBL height (white line) and vertical wind speeds during the winter season. As a result of this phenomenon, normal vertical convective mixing and a typical PBL height were possible. In other words, the PBL quickly reduces after sunset due to a decrease in thermals rising from the surface.

4. Discussion

Due to their high emissivity and solar reflectance, PDRC materials can radiate sufficient heat to steadily remain up to 5–10 °C cooler than the surrounding $T_{ambient}$, even during typical mid-summer day [13,62,63]. PDRC materials present an excellent cooling

performance during the warm periods; nevertheless, they are a serious concern during the winter. Their use in the urban environment could decrease the urban ambient temperature during the cold season and increase the heating needs of buildings. Applying conventional PDRC materials in a tropical city (the Kolkata Metropolitan Area) decreased the daily ambient temperature in winter up to 1.1 °C and 0.8 °C during daytime and nighttime, respectively. Although their overcooling penalty is considerably lower than their summer cooling contribution, it is an undesirable effect that may limit the broad application of this technology in certain cities. To overcome the unwanted side effect of the winter overcooling penalty, optical modulation of their reflectance and emissivity is proposed. By introducing an additional tunable layer to the PDRC materials, it is possible to modify their solar reflectance and emissivity during the cold period without compromising their summer cooling efficiency. Initial research has shown that seasonal switching of their optical properties is technically feasible using a spectrum of potential technical solutions. The simulations with reflectivity and emissivity modulated PDRC (ρ+ε) showed that the daily ambient temperature in winter could be increased up to 0.4 °C and 1.4 °C during the daytime and nighttime, respectively.

PDRC materials need to be further developed for integration into roofing systems. For example, non-modulated PDRC materials might be more beneficial in locations with almost no heating period, experiencing extreme summers and temperate winters. In contrast, the modulated PDRC materials could be more suitable in some temperate climates that experience heating seasons during the winter. Moreover, research should analyze the aging caused by weathering, soiling, and biological growth that can alter the radiative properties of these materials as part of roofing systems. Aging could deteriorate the high reflectivity of the materials, increasing the roof surface temperature and, as a result, reducing the cooling load savings. Finally, when discussing modulated PDRC, the reversibility of the tunable layer and its durability should be determined.

Finally, besides studying PDRC as an overheating solution, their energy saving potential should also be studied. To do so, the optimal insulation thickness should be determined for each location and orientation to observe any potential internal benefit. Careful study of the insulation thicknesses should be made as too much insulation could hinder any beneficial impact on the interior temperatures. To conclude, when modulation techniques are included, PDRC materials are an excellent strategy for urban planning to mitigate urban overheating across climates.

5. Conclusions

In this research, we simulated standard passive daytime radiative coolers (PDRC) and three other PDRC materials with modulated reflectivity, emissivity, and both reflectivity and emissivity. A mesoscale climate model can effectively run these scenarios for large-scale testing. Thus, the following conclusions can be attained:

1. Solar reflectance (ρ) or emissivity (ε) modulation of the PDRC materials has insignificant mitigation potential for the overcooling penalty, both during the day and night.
2. Reflectivity and emissivity modulated PDRC materials increase their daily maximum latent heat by 182 Wm^{-2} and their daily maximum heat storage by 244 Wm^{-2}, compared to the non-modulated PDRC materials.
3. When both the reflectivity and the emissivity (ρ+ε) are modulated, a positive energy balance occurs during the winter period, as the surface temperature of the materials ($T_{surface}$) may increase up to 0.9 °C compared to the control case. This results in an ambient temperature rise of 0.4 °C and 1.5 °C when compared to the CTRL and the conventional PDRC materials, respectively.
4. Optically modulated PDRC materials can be an excellent urban heat mitigation technology for use during the summer period without leading to an overcooling penalty during the winter.

Future work is ongoing to develop and integrate modulation technologies into PDRC materials. However, the success of this technology is firmly linked to scalability, spectral

variability, cost-effectiveness, durability, and tunability, much more than to suboptimal properties. Increasing the scalability of broadband radiative structures and shrinking their fabrication cost is essential to further endorse and enhance their use for heat mitigation purposes. Low-cost optically modulated passive systems are currently under development. They are expected to be commercially available on the market soon with high future potential to reduce urban heat in cities without leading to an overcooling penalty during cold periods.

Author Contributions: A.K.: software, methodology, validation, formal analysis, writing—original draft preparation; L.C.: investigation, writing—original draft preparation; J.F.: investigation, writing—original draft preparation; S.K.: software, formal analysis, writing—review and editing; R.K.: data curation, validation, writing—review and editing; Q.-V.D.: software, formal analysis, writing—review and editing; M.S.: conceptualization, project administration, supervision, writing—review and editing. All authors have read and agreed to the published version of the manuscript.

Funding: This research received no external funding.

Institutional Review Board Statement: Not applicable.

Data Availability Statement: The data that support the findings of this study are available from the corresponding author upon reasonable request. The source code of the WRF model, Version 4.0 used in this paper can be downloaded from https://www2.mmm.ucar.edu/wrf/users/downloads.html accessed on 24 October 2020. Codes used to set up model simulations, analyze data, and create figures can be provided upon request from the corresponding author.

Conflicts of Interest: The authors declare no conflict of interest.

References

1. Founda, D.; Santamouris, M. Synergies between Urban Heat Island and Heat Waves in Athens (Greece), during an Extremely Hot Summer (2012). *Sci. Rep.* **2017**, *7*, 10973. [CrossRef] [PubMed]
2. Santamouris, M. Innovating to Zero the Building Sector in Europe: Minimising the Energy Consumption, Eradication of the Energy Poverty and Mitigating the Local Climate Change. *Sol. Energy* **2016**, *128*, 61–94. [CrossRef]
3. Santamouris, M. Analyzing the Heat Island Magnitude and Characteristics in One Hundred Asian and Australian Cities and Regions. *Sci. Total Environ.* **2015**, *512–513*, 582–598. [CrossRef] [PubMed]
4. Santamouris, M. Recent Progress on Urban Overheating and Heat Island Research. Integrated Assessment of the Energy, Environmental, Vulnerability and Health Impact. Synergies with the Global Climate Change. *Energy Build.* **2020**, *207*, 109482. [CrossRef]
5. Santamouris, M. On the Energy Impact of Urban Heat Island and Global Warming on Buildings. *Energy Build.* **2014**, *82*, 100–113. [CrossRef]
6. Santamouris, M.; Cartalis, C.; Synnefa, A.; Kolokotsa, D. On the Impact of Urban Heat Island and Global Warming on the Power Demand and Electricity Consumption of Buildings—A Review. *Energy Build.* **2015**, *98*, 119–124. [CrossRef]
7. Shishegar, N. Street Design and Urban Microclimate: Analyzing the Effects of Street Geometry and Orientation on Airflowand Solar Access in Urban Canyons. *J. Clean Energy Technol.* **2013**, *1*, 52–56. [CrossRef]
8. Oliveira Panão, M.J.N.; Gonçalves, H.J.P.; Ferrão, P.M.C. Numerical Analysis of the Street Canyon Thermal Conductance to Improve Urban Design and Climate. *Build. Environ.* **2009**, *44*, 177–187. [CrossRef]
9. Georgakis, C.; Santamouris, M. Experimental Investigation of Air Flow and Temperature Distribution in Deep Urban Canyons for Natural Ventilation Purposes. *Energy Build.* **2006**, *38*, 367–376. [CrossRef]
10. Akbari, H.; Cartalis, C.; Kolokotsa, D.; Muscio, A.; Pisello, A.L.; Rossi, F.; Santamouris, M.; Synnefa, A.; Wong, N.H.; Zinzi, M. Local Climate Change and Urban Heat Island Mitigation Techniques—The State of the Art. *J. Civ. Eng. Manag.* **2016**, *22*, 1–16. [CrossRef]
11. Santamouris, M.; Yun, G.Y. Recent Development and Research Priorities on Cool and Super Cool Materials to Mitigate Urban Heat Island. *Renew. Energy* **2020**, *161*, 792–807. [CrossRef]
12. Santamouris, M.; Feng, J. Recent Progress in Daytime Radiative Cooling: Is It the Air Conditioner of the Future? *Buildings* **2018**, *8*, 168. [CrossRef]
13. Raman, A.P.; Anoma, M.A.; Zhu, L.; Rephaeli, E.; Fan, S. Passive Radiative Cooling below Ambient Air Temperature under Direct Sunlight. *Nature* **2014**, *515*, 540–544. [CrossRef] [PubMed]
14. Hossain, M.M.; Jia, B.; Gu, M. A Metamaterial Emitter for Highly Efficient Radiative Cooling. *Adv. Opt. Mater.* **2015**, *3*, 1047–1051. [CrossRef]
15. Kecebas, M.A.; Menguc, M.P.; Kosar, A.; Sendur, K. Passive Radiative Cooling Design with Broadband Optical Thin-Film Filters. *J. Quant. Spectrosc. Radiat. Transf.* **2017**, *198*, 179–186. [CrossRef]

16. Wu, D.; Liu, C.; Xu, Z.; Liu, Y.; Yu, Z.; Yu, L.; Chen, L.; Li, R.; Ma, R.; Ye, H. The Design of Ultra-Broadband Selective near-Perfect Absorber Based on Photonic Structures to Achieve near-Ideal Daytime Radiative Cooling. *Mater. Des.* **2018**, *139*, 104–111. [CrossRef]
17. Atiganyanun, S.; Plumley, J.B.; Han, S.J.; Hsu, K.; Cytrynbaum, J.; Peng, T.L.; Han, S.M.; Han, S.E. Effective Radiative Cooling by Paint-Format Microsphere-Based Photonic Random Media. *ACS Photonics* **2018**, *5*, 1181–1187. [CrossRef]
18. Aili, A.; Wei, Z.; Chen, Y.; Zhao, D.; Yang, R.; Yin, X. Selection of Polymers with Functional Groups for Day-Time Radiative Cooling. *Mater. Today Phys.* **2019**, *10*, 100127. [CrossRef]
19. Zhai, Y.; Ma, Y.; David, S.N.; Zhao, D.; Lou, R.; Tan, G.; Yang, R.; Yin, X. Scalable-Manufactured Randomized Glass-Polymer Hybrid Metamaterial for Daytime Radiative Cooling. *Science* **2017**, *355*, 1062–1066. [CrossRef] [PubMed]
20. Carlosena, L.; Andueza, Á.; Torres, L.; Irulegi, O.; Hernández-Minguillón, R.J.; Sevilla, J.; Santamouris, M. Experimental Development and Testing of Low-Cost Scalable Radiative Cooling Materials for Building Applications. *Sol. Energy Mater. Sol. Cells* **2021**, *230*, 111209. [CrossRef]
21. Mandal, J.; Fu, Y.; Overvig, A.; Jia, M.; Sun, K.; Shi, N.; Zhou, H.; Xiao, X.; Yu, N.; Yang, Y. Hierarchically Porous Polymer Coatings for Highly Efficient Passive Daytime Radiative Cooling. *Science* **2018**, *362*, 315–319. [CrossRef] [PubMed]
22. Ao, X.; Hu, M.; Zhao, B.; Chen, N.; Pei, G.; Zou, C. Preliminary Experimental Study of a Specular and a Diffuse Surface for Daytime Radiative Cooling. *Sol. Energy Mater. Sol. Cells* **2019**, *191*, 290–296. [CrossRef]
23. Feng, J.; Gao, K.; Santamouris, M.; Shah, K.W.; Ranzi, G. Dynamic Impact of Climate on the Performance of Daytime Radiative Cooling Materials. *Sol. Energy Mater. Sol. Cells* **2020**, *208*, 110426. [CrossRef]
24. Yin, X.; Yang, R.; Tan, G.; Fan, S. Terrestrial Radiative Cooling: Using the Cold Universe as a Renewable and Sustainable Energy Source. *Science* **2020**, *370*, 786–791. [CrossRef] [PubMed]
25. Bartesaghi-Koc, C.; Haddad, S.; Pignatta, G.; Paolini, R.; Prasad, D.; Santamouris, M. Can Urban Heat Be Mitigated in a Single Urban Street? Monitoring, Strategies, and Performance Results from a Real Scale Redevelopment Project. *Sol. Energy* **2021**, *216*, 564–588. [CrossRef]
26. Baniassadi, A.; Heusinger, J.; Sailor, D.J. Building Energy Savings Potential of a Hybrid Roofing System Involving High Albedo, Moisture Retaining Foam Materials. *Energy Build.* **2018**, *169*, 283–294. [CrossRef]
27. Khan, A.; Carlosena, L.; Khorat, S.; Khatun, R.; Doan, Q.-V.; Feng, J.; Santamouris, M. On the Winter Overcooling Penalty of Super Cool Photonic Materials in Cities. *Sol. Energy Adv.* **2021**, *1*, 100009. [CrossRef]
28. Ji, H.; Liu, D.; Cheng, H.; Zhang, C.; Yang, L. Vanadium Dioxide Nanopowders with Tunable Emissivity for Adaptive Infrared Camouflage in Both Thermal Atmospheric Windows. *Sol. Energy Mater. Sol. Cells* **2018**, *175*, 96–101. [CrossRef]
29. Ono, M.; Chen, K.; Li, W.; Fan, S. Self-Adaptive Radiative Cooling Based on Phase Change Materials. *Opt. Express* **2018**, *26*, A777. [CrossRef] [PubMed]
30. Lang, F.; Wang, H.; Zhang, S.; Liu, J.; Yan, H. Review on Variable Emissivity Materials and Devices Based on Smart Chromism. *Int. J. Thermophys.* **2017**, *39*, 6. [CrossRef]
31. Jorgenson, G.V.; Lee, J.C. Doped Vanadium Oxide for Optical Switching Films. *Sol. Energy Mater.* **1986**, *14*, 205–214. [CrossRef]
32. Tazawa, M.; Jin, P.; Tanemura, S. Thin Film Used to Obtain a Constant Temperature Lower than the Ambient. *Thin Solid Films* **1996**, *281–282*, 232–234. [CrossRef]
33. Santos, A.J.; Lacroix, B.; Domínguez, M.; García, R.; Martin, N.; Morales, F.M. Controlled Grain-Size Thermochromic VO2 Coatings by the Fast Oxidation of Sputtered Vanadium or Vanadium Oxide Films Deposited at Glancing Angles. *Surf. Interfaces* **2021**, *27*, 101581. [CrossRef]
34. Li, B.; Yao, J.; Tian, S.; Fang, Z.; Wu, S.; Liu, B.; Gong, X.; Tao, H.; Zhao, X. A Facile One-Step Annealing Route to Prepare Thermochromic W Doped VO2(M) Particles for Smart Windows. *Ceram. Int.* **2020**, *46*, 18274–18280. [CrossRef]
35. Nazari, S.; Charpentier, P.A. Sol-Gel Processing of VO_2 (M) in Supercritical CO_2 and Supercritical CO_2/Ionic Liquid Biphasic System. *J. Supercrit. Fluids* **2020**, *165*, 104989. [CrossRef]
36. Zhao, X.P.; Mofid, S.A.; Gao, T.; Tan, G.; Jelle, B.P.; Yin, X.B.; Yang, R.G. Durability-Enhanced Vanadium Dioxide Thermochromic Film for Smart Windows. *Mater. Today Phys.* **2020**, *13*, 100205. [CrossRef]
37. Zhao, Z.; Liu, Y.; Wang, D.; Ling, C.; Chang, Q.; Li, J.; Zhao, Y.; Jin, H. Sn Dopants Improve the Visible Transmittance of VO_2 Films Achieving Excellent Thermochromic Performance for Smart Window. *Sol. Energy Mater. Sol. Cells* **2020**, *209*, 110443. [CrossRef]
38. Granqvist, C.G.; Lansåker, P.C.; Mlyuka, N.R.; Niklasson, G.A.; Avendaño, E. Progress in Chromogenics: New Results for Electrochromic and Thermochromic Materials and Devices. *Sol. Energy Mater. Sol. Cells* **2009**, *93*, 2032–2039. [CrossRef]
39. Kanu, S.S.; Binions, R. Thin Films for Solar Control Applications. *Proc. R. Soc. Math. Phys. Eng. Sci.* **2010**, *466*, 19–44. [CrossRef]
40. Perez, G.; Allegro, V.R.; Corroto, M.; Pons, A.; Guerrero, A. Smart Reversible Thermochromic Mortar for Improvement of Energy Efficiency in Buildings. *Constr. Build. Mater.* **2018**, *186*, 884–891. [CrossRef]
41. Wong, R.Y.M.; Tso, C.Y.; Chao, C.Y.H.; Huang, B.; Wan, M.P. Ultra-Broadband Asymmetric Transmission Metallic Gratings for Subtropical Passive Daytime Radiative Cooling. *Sol. Energy Mater. Sol. Cells* **2018**, *186*, 330–339. [CrossRef]
42. Mandal, J.; Du, S.; Dontigny, M.; Zaghib, K.; Yu, N.; Yang, Y. $Li_4Ti_5O_{12}$: A Visible-to-Infrared Broadband Electrochromic Material for Optical and Thermal Management. *Adv. Funct. Mater.* **2018**, *28*, 1802180. [CrossRef]
43. Mandal, J.; Jia, M.; Overvig, A.; Fu, Y.; Che, E.; Yu, N.; Yang, Y. Porous Polymers with Switchable Optical Transmittance for Optical and Thermal Regulation. *Joule* **2019**, *3*, 3088–3099. [CrossRef]

44. Tang, K.; Dong, K.; Li, J.; Gordon, M.P.; Reichertz, F.G.; Kim, H.; Rho, Y.; Wang, Q.; Lin, C.-Y.; Grigoropoulos, C.P.; et al. Temperature-Adaptive Radiative Coating for All-Season Household Thermal Regulation. *Science* **2021**, *374*, 1504–1509. [CrossRef] [PubMed]
45. Xue, X.; Qiu, M.; Li, Y.; Zhang, Q.M.; Li, S.; Yang, Z.; Feng, C.; Zhang, W.; Dai, J.-G.; Lei, D.; et al. Creating an Eco-Friendly Building Coating with Smart Subambient Radiative Cooling. *Adv. Mater.* **2020**, *32*, 1906751. [CrossRef]
46. Wang, S.; Jiang, T.; Meng, Y.; Yang, R.; Tan, G.; Long, Y. Scalable Thermochromic Smart Windows with Passive Radiative Cooling Regulation. *Science* **2021**, *374*, 1501–1504. [CrossRef] [PubMed]
47. IPCC. *Climate Change 2021: The Physical Science Basis. Contribution of Working Group I to the Sixth Assessment Report of the Intergovernmental Panel on Climate Change*; Masson-Delmotte, V., Zhai, P., Pirani, A., Connors, S.L., Péan, C., Berger, S., Caud, N., Chen, Y., Goldfarb, L., Gomis, M.I., et al., Eds.; Cambridge University Press: Cambridge, MA, USA; Cambridge, UK, in press.
48. Dhorde, A. Long-Term Temperature Trends at Four Largest Cities of India during the Twentieth Century. *J. Ind. Geophys. Union* **2009**, *13*, 85–97.
49. Kothawale, D.R.; Deshpande, N.R.; Kolli, R.K. Long Term Temperature Trends at Major, Medium, Small Cities and Hill Stations in India during the Period 1901–2013. *Am. J. Clim. Chang.* **2016**, *5*, 383–398. [CrossRef]
50. Feng, J.; Khan, A.; Doan, Q.-V.; Gao, K.; Santamouris, M. The Heat Mitigation Potential and Climatic Impact of Super-Cool Broadband Radiative Coolers on a City Scale. *Cell Rep. Phys. Sci.* **2021**, *2*, 100485. [CrossRef]
51. Skamarock, W.C.; Klemp, J.B.; Dudhia, J.; Gill, D.O.; Liu, Z.; Berner, J.; Wang, W.; Powers, J.G.; Duda, M.G.; Barker, D.M.; et al. *A Description of the Advanced Research WRF Model Version 4*; UCAR/NCAR; National Center for Atmospheric Research: Boulder, CO, USA, 2019.
52. Chen, F.; Kusaka, H.; Bornstein, R.; Ching, J.; Grimmond, C.S.B.; Grossman-Clarke, S.; Loridan, T.; Manning, K.W.; Martilli, A.; Miao, S.; et al. The Integrated WRF/Urban Modelling System: Development, Evaluation, and Applications to Urban Environmental Problems. *Int. J. Climatol.* **2011**, *31*, 273–288. [CrossRef]
53. Kusaka, H.; Kondo, H.; Kikegawa, Y.; Kimura, F. A Simple Single-Layer Urban Canopy Model For Atmospheric Models: Comparison With Multi-Layer And Slab Models. *Bound.-Layer Meteorol.* **2001**, *101*, 329–358. [CrossRef]
54. Dudhia, J. Numerical Study of Convection Observed during the Winter Monsoon Experiment Using a Mesoscale Two-Dimensional Model. *J. Atmos. Sci.* **1989**, *46*, 3077–3107. [CrossRef]
55. Mlawer, E.J.; Taubman, S.J.; Brown, P.D.; Iacono, M.J.; Clough, S.A. Radiative Transfer for Inhomogeneous Atmospheres: RRTM, a Validated Correlated-k Model for the Longwave. *J. Geophys. Res. Atmos.* **1997**, *102*, 16663–16682. [CrossRef]
56. Lin, Y.-L.; Farley, R.D.; Orville, H.D. Bulk Parameterization of the Snow Field in a Cloud Model. *J. Appl. Meteorol. Climatol.* **1983**, *22*, 1065–1092. [CrossRef]
57. Mellor, G.L.; Yamada, T. A hierarchy of turbulence closure models for planetary boundary layers. *J. Atmos. Sci.* **1974**, *31*, 1791–1806. [CrossRef]
58. Kain, J.S. The Kain–Fritsch Convective Parameterization: An Update. *J. Appl. Meteorol. Climatol.* **2004**, *43*, 170–181. [CrossRef]
59. Pleim, J.E. A Combined Local and Nonlocal Closure Model for the Atmospheric Boundary Layer. Part I: Model Description and Testing. *J. Appl. Meteorol. Climatol.* **2007**, *46*, 1383–1395. [CrossRef]
60. Karlessi, T.; Santamouris, M. Improving the Performance of Thermochromic Coatings with the Use of UV and Optical Filters Tested under Accelerated Aging Conditions. *Int. J. Low-Carbon Technol.* **2013**, *10*, 45–61. [CrossRef]
61. Carlosena, L.; Ruiz-Pardo, Á.; Feng, J.; Irulegi, O.; Hernández-Minguillón, R.J.; Santamouris, M. On the Energy Potential of Daytime Radiative Cooling for Urban Heat Island Mitigation. *Sol. Energy* **2020**, *208*, 430–444. [CrossRef]
62. Leroy, A.; Bhatia, B.; Kelsall, C.C.; Castillejo-Cuberos, A.; Di Capua H, M.; Zhao, L.; Zhang, L.; Guzman, A.M.; Wang, E.N. High-Performance Subambient Radiative Cooling Enabled by Optically Selective and Thermally Insulating Polyethylene Aerogel. *Sci. Adv.* **2019**, *5*, eaat9480. [CrossRef]
63. Zhao, D.; Aili, A.; Zhai, Y.; Xu, S.; Tan, G.; Yin, X.; Yang, R. Radiative Sky Cooling: Fundamental Principles, Materials, and Applications. *Appl. Phys. Rev.* **2019**, *6*, 021306. [CrossRef]